# Facile Synthesis of Water-Dispersible Conducting Polymer Nanospheres

**Yaozu Liao,[†,‡] Xin-Gui Li,[‡,*] and Richard B. Kaner[†,*]**

[†]Department of Chemistry & Biochemistry and California NanoSystems Institute, University of California, Los Angeles, Los Angeles, California 90095-1569 and [‡]Institute of Materials Chemistry, College of Materials Science and Engineering, Tongji University, 1239 Si-Ping Road, Shanghai 200092, China

**ABSTRACT** Water-dispersible polypyrrole nanospheres with diameters of less than 100 nm were synthesized in high yield without any templates, surfactants, or functional dopants by the introduction of 2,4-diaminodiphenylamine as an initiator into a reaction mixture of pyrrole monomer, oxidant, and acid. The initiator plays a critical role in tailoring the nanostructures of polypyrrole. 2,4-Diaminodiphenylamine interacts with acid to form cations, which combine with various anions to self-assemble resulting in different size nanomicelles. These nanomicelles, stabilized by initiator molecules, act as templates to encapsulate pyrrole and oxidant leading to the formation of nanospheres during polymerization. When smaller acids are used, smaller diameter sphere-like polypyrrole nanostructures are obtained. The as-synthesized polypyrrole nanospheres can then be used to fabricate highly conducting nitrogen-doped carbon nanospheres with controllable sizes of 50—220 nm with monodispersities up to 95% after pyrolysis. The size of the carbon nanospheres decreases by 20—30 nm due to carbonization when compared to the original polymer nanospheres. The molecular structures, morphologies, and electrical properties along with the formation mechanism of the polypyrrole and carbon nanospheres are discussed.

**KEYWORDS:** conducting polymers · carbon · nanoparticles · self-assembly · synthesis

Since their discovery over thirty years ago, intrinsically conducting polymers have shown great potential for a variety of applications including sensors, anticorrosion coatings, batteries, capacitors, actuators, and optical devices.[1−3] As one of the leading conducting polymers, polypyrrole shows promise for commercial applications because of its simple synthesis, high conductivity, environmental stability, and biocompatibility.[4−7] Polypyrrole composites have been shown to exhibit biodegradability which could lead to biomedical applications such as in drug delivery or as scaffolds for tissue engineering.[7] Processability is arguably the biggest problem for utilization of this conducting polymer. A great deal of research has been directed toward preparation and fabrication of nanostructured polypyrrole in the form of nanoparticles, nanofibers, nanotubes, nanorods, and nanowires to improve its processability and widen its applications. Examples include template assisted synthesis,[8−12] seeded growth,[13] functional dopant-induced processing,[14,15] and emulsion,[16−23] dispersion,[24,25] and interfacial polymerizations.[26−28] Despite the variety of synthetic methods reported, the synthesis of polypyrrole nanostructures have met with only limited success. The main disadvantages of template and seeded growth synthetic routes are that the template or seeds add cost and complexity to the synthesis, and removing the template or seeds often affects the alignment and physical properties of the nanostructures. Emulsion and dispersion polymerizations often need external emulsifiers or stabilizers, which can be difficult to remove.

The discovery of new nanostructured carbon materials including fullerenes,[29] nanotubes,[30] nanofibers,[31] as well as nanocones,[32] has sparked tremendous research efforts into the study of carbon-based materials because of their unique electronic, mechanical, thermal, chemical, and physical properties. Additionally, carbon nanospheres have attracted great interest for potential applications as high density/high strength fillers,[33] lithium-ion battery electrodes,[34] lithium storage,[35,36] adsorbents,[37] cell delivery,[38,39] and as supports for catalytic systems.[40] Various methods have been proposed for the synthesis of carbon nanospheres including chemical vapor deposition,[41,42] laser-induced pyrolysis,[43,44] arc-discharge,[45] and templated growth.[46] Drawbacks to these methods include the metal catalysts often end up incorporated into the carbon nanospheres and the need for complex equipment.

Therefore, simple rapid methods for the synthesis of water-dispersible polypyrrole and carbon nanospheres are of broad

*Address correspondence to kaner@chem.ucla.edu, adamxgli@yahoo.com.

Received for review June 18, 2010 and accepted August 26, 2010.

**Published online September 7, 2010.** 10.1021/nn101378p

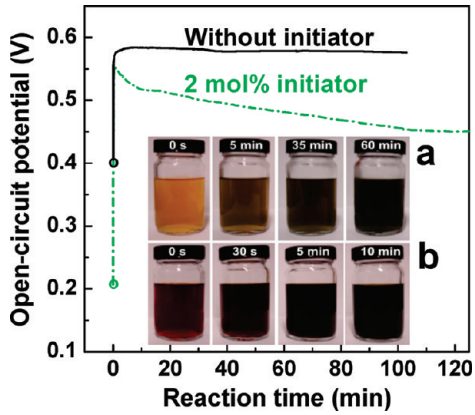


**Figure 1. Open circuit potential (OCP) measurements of the polymerization of pyrrole at 0 °C without an initiator (solid line) and with 2 mol % of the 2,4-diaminodiphenylamine initiator (dotted line). Note that the reaction carried out with the initiator has a lower starting potential. The inset shows images of polypyrrole synthesis (a) without and (b) with 2 mol % of the initiator taken at different time intervals.**

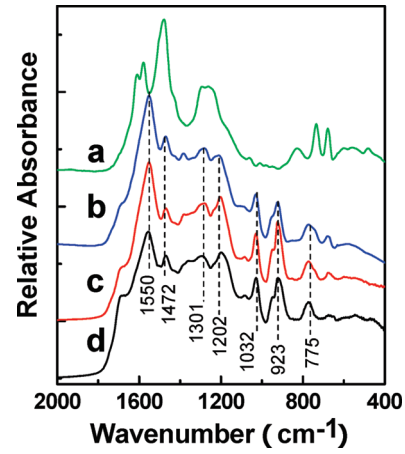


**Figure 2. FT-IR spectra of (a) oligomeric 2,4-diaminodiphenylamine and (b−d) polypyrrole synthesized with 2,4-diaminodiphenylamine as an initiator in the following concentrations: (b) 10 mol %, (c) 2 mol %, and (d) 0 mol %.**

interest. In our previous work, polypyrrole nanofibers were successfully synthesized by introducing bipyrrole as an initiator.[47,48] Here we explore a rapid initiated polymerization to synthesize highly dispersible polypyrrole nanospheres with 2,4-diaminodiphenylamine as an initiator in aqueous solution. We find that the size and morphology of these polypyrrole nanospheres can be tuned by controlling the following reaction parameters: (1) the initiator concentration, (2) the oxidant used, and (3) the acid employed. An interesting discovery with the as-synthesized nanostructured polypyrrole is that it provides an excellent precursor for the growth of nitrogen-doped carbon nanospheres. Surprisingly, the conductivity of these carbon nanospheres approaches that of many metallic conductors. This paper therefore provides a simple rapid route to produce highly quality, uniform conducting polymer nanospheres in a scalable process. The materials can be readily converted to carbon nanospheres and scaled up if desired.

## RESULTS AND DISCUSSION

**Synthesis and Structural Determination of Polypyrrole Nanospheres.** When pyrrole is chemically polymerized using $FeCl_3$ as the oxidant, the addition of 2 mol % of the initiator 2,4-diaminodiphenylamine leads to a much lower starting potential (0.2 V) than when the reaction is carried out without the initiator (0.4 V) (Figure 1). The reaction mixture darkens quickly and polypyrrole precipitates are observed within 30 s, as opposed to about an hour for a reaction performed in the absence of an initiator (Figure 1, insets). This signifies that the initiator accelerates the reaction rate. The initiator likely copolymerizes with pyrrole in the initial stages of polymerization, acting like bipyrrole which promotes homogeneous nucleation of polypyrrole chains, since they both have lower starting potentials (0.2 and 0.1 V), respectively, *versus* 0.4 V for pyrrole, as confirmed by open circuit potential (OCP) measurements.[47] Structural determination of the as-synthesized polypyrrole was carried out by Fourier transform infrared (FT-IR) spectroscopy, ultraviolet−visible (UV−vis) spectroscopy, and elemental analysis. Comparison of the FT-IR spectra of polypyrrole nanospheres synthesized using two different concentrations of initiator with the spectrum of oligomeric 2,4-diaminodiphenylamine shows distinct differences, such as the absence of bands at 740, 1032, 1480, and 1580 $cm^{-1}$ for the oligomeric initiator (Figure 2). Spectra of polypyrrole synthesized with an initiator indicate that stretching bands for the pyrrole ring occur at 1472 and 1550 $cm^{-1}$,[12,19] a shoulder peak that can be attributed to part of the oxidized pyrrole ring at 1690 $cm^{-1}$,[49] stretching bands for C−N at 1032 and 1301 $cm^{-1}$,[50] and stretching bands for doped polypyrrole at 923 and 1202 $cm^{-1}$.[51] Note that a small shoulder FT-IR peak at 740 $cm^{-1}$ confirms that a small amount of 2,4-diaminodiphenylamine has copolymerized with pyrrole. The products obtained with the initiator exhibit two typical UV−vis absorptions around 460 nm and above 900 nm, which can be assigned to the transitions from the valence band to the antibonding and bonding polaron state of doped polypyrrole, respectively (Supporting Information, Figure S1).[19] Elemental analysis reveals the presence of C (55.0 wt %), N (16.3 wt %), and H (4.5 wt %) in polypyrrole nanospheres synthesized with 10 mol % initiator. The C/N ratio of the polypyrrole nanospheres (3.38) is consistent with the theoretical C/N ratio of pure polypyrrole (3.43).[47] These results indicate that the chemical composition of the observed polypyrrole nanospheres is very similar to that of conventional polypyrrole.

**Size and Morphologies of Dispersible Polypyrrole Nanospheres.** As measured by dynamic light scattering (DLS), the number-average diameters ($D_n$) of the as-synthesized polypyrrole particles dispersed in methanol decrease from 1200 to 280 nm when the initiator concentration

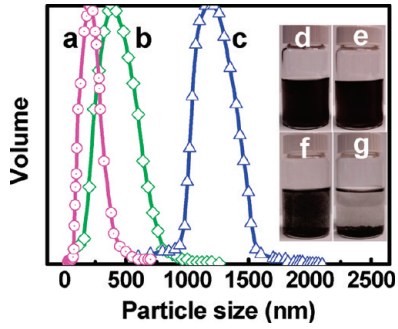


**Figure 3. Size distributions of polypyrrole particles produced using the initiator 2,4-diaminodiphenylamine at (a) 10 mol %, (b) 2 mol %, and (c) without the initiator. The insets (d−g) show photographs illustrating the stability of the polypyrrole dispersions in methanol (0.5 g/L): (d) synthesized with 10 mol % initiator, (e) panel d after 24 h, (f) synthesized without the initiator, and (g) panel f after 5 h.**

is increased from 0 to 10 mol % (Figure 3). The size of the polypyrrole nanospheres changes little with further increases in the concentration of the initiator. Note that the diameters of the polypyrrole nanospheres can be tuned by choosing different size doping acids. For example, when the reaction was performed in the presence of camphorsulfonic acid (CSA), perchloric acid ($HClO_4$), nitric acid ($HNO_3$), and hydrochloric acid (HCl), the $D_n$ of the as-synthesized nanospheres varied from 220, to 200, to 110, to 85 nm.

Investigating the stability of polypyrrole dispersions in methanol reveals a striking contrast between materials synthesized with and without the initiator (Figure 3, insets). For reactions performed in the absence of the initiator, the as-synthesized polypyrrole exhibits irregularly shaped agglomerates along with some big sheets measuring several micrometers, which mostly precipitate within 5 h. However, upon introduction of 10 mol % of the initiator into the reaction mixture, the as-synthesized product does not aggregate or settle out from the dispersion even after standing for 24 h. Surprisingly, this polymer dispersion is completely stable in methanol for at least 3 months. Note that the as-synthesized polypyrrole nanospheres are dispersible in many polar solvents including DI water, ethanol, acetone, toluene, and 1-methyl-2-pyrrolidinone.

To figure out the stabilization mechanism for these aqueous suspensions, electrophoretic mobility and zeta potential measurements were carried out at a pH of ~4.5. The electrophoretic mobility and zeta potential of polypyrrole particles synthesized without the initiator are $(3.66 \pm 0.06) \times 10^8$ m$^2$/(V·s) and 46.83 ± 0.80 mV, which increased to $(4.37 \pm 0.04) \times 10^8$ m$^2$/(V·s) and 55.85 ± 0.51 mV, respectively, when the initiator was added. The enhanced charge may be due the initiator when copolymerized with pyrrole forming ammonium ion-like groups in the presence of acid. According to the well-known Derjaguin−Landau−Verwey−Overbeek (DLVO) theory, the stability of colloidal suspensions depends on potential energy curves which are the sum of two contributions, the van der Waals force and the electrostatic force, relative to the free energy of interactions. Greater positive charge or negative charge leads to more dispersible and stable colloidal suspensions. The large ammonium ion-like groups could be also act as steric stabilizers. Thus both charge and steric-based stabilizer functions of the initiator help explain why the polypyrrole nanospheres are highly dispersible and the resulting suspensions so stable.

Morphologies of polypyrrole nanospheres dispersed in DI water as determined by SEM and TEM demonstrate clear differences in size and morphology when synthesized in the absence and presence of the initiator (Figure 4a,b). For reactions performed without the initiator, irregularly shaped aggregates with diameters of >600 nm predominate. However, upon introduction of the initiator, a significant change is observed from irregularly shaped agglomerates to smooth nanospheres.

The size of the nanospheres (80−300 nm) is not only controlled by the initiator concentraton (as determined by DLS), but also tuned by the oxidant and the doping acid employed. When $FeCl_3$ is used as the oxidant, well-defined polypyrrole nanospheres are obtained (Figure 4b). When ammonium peroxydisulfate (APS) is employed, the polypyrrole forms nanoaggregates (Figure 4c). When potassium dichromate ($K_2Cr_2O_7$) is utilized, the polypyrrole readily forms nanostructures with average diameters of 90 nm and lengths of 200 nm (Figure 4d). Note that the oxidation potentials (OP) of APS, $FeCl_3$, and $K_2Cr_2O_7$ in water (without acid present) follow the order: $OP_{APS} = 2.0\ V > OP_{FeCl_3} = 0.77\ V > OP_{K_2Cr_2O_7} = \sim 0.1\ V$, which suggests that the growth and elongation process for the polypyrrole particles oxidized with $K_2Cr_2O_7$ is much slower than that with APS. While adding initiator promotes homogeneous nucleation of polypyrrole chains, when too much oxidant is added, heterogeneous nucleation results. This makes the diameter of particles oxidized by $K_2Cr_2O_7$ smaller than that produced by APS, while the diameter of polypyrrole particles oxidized by $FeCl_3$ falls in between. At the same time, the oxidants also affect the conductivity of the products. Although smaller diameter and more dispersible polypyrrole was obtained using $K_2Cr_2O_7$, we found that $FeCl_3$ with an intermediate OP is the best oxidant for producing polypyrrole nanospheres with high conductivity and good dispersibility.

The size of the polypyrrole nanospheres can be adjusted by choosing doping acids with different size anions (*e.g.*, the radius of $CSA^- = 3.07$ Å > $ClO_4^- = 2.36$ Å > $NO_3^- = 1.89$ Å > $Cl^- = 1.78$ Å).[52,53] SEM images confirm that upon introduction of the relatively small size dopants HCl or $HNO_3$, the polypyrrole nanospheres obtained have $D_n$ around 100 and 120 nm, respectively (Figure 5c,d). In contrast, the size of the polypyrrole nanospheres increases to 150−250 nm when the larger doping acids CSA and $HClO_4$ are used (Figure 5a,b).

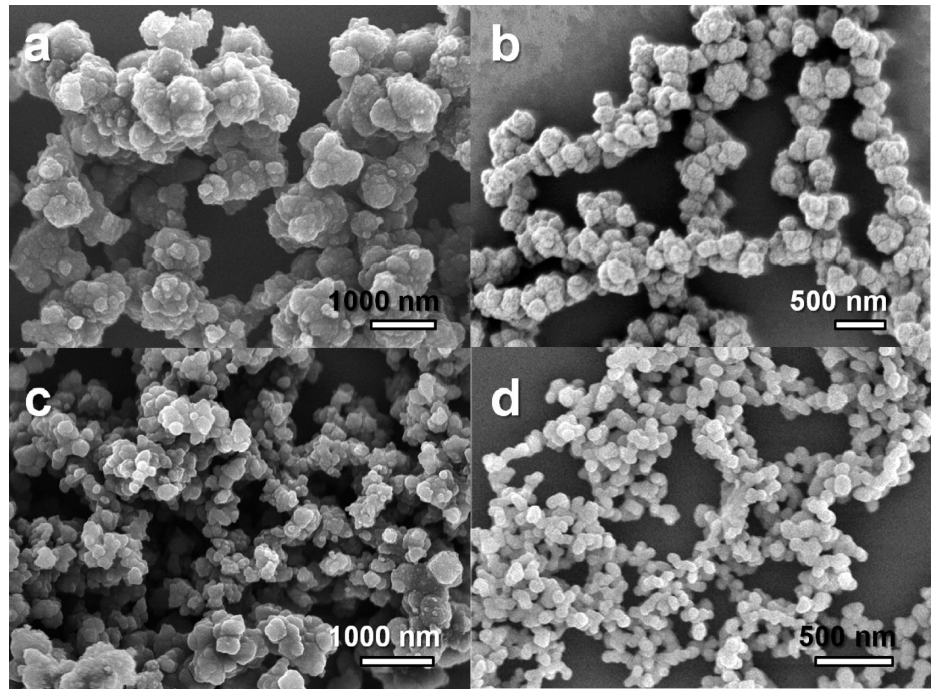


**Figure 4. SEM images of polypyrrole synthesized (a) without initiator using $FeCl_3$ as the oxidant and (b–d) with 10 mol % 2,4-diaminodiphenylamine initiator using the following oxidants: (b) $FeCl_3$, (c) APS, and (d) $K_2Cr_2O_7$ without any acid.**

The sheet resistance of the as-synthesized polypyrrole nanospheres is $3.1 \times 10^4$ Ω/□ when the synthesis was carried out without acids using $FeCl_3$ as the oxidant. The sheet resistance decreased to $2.9 \times 10^2$ Ω/□ when the polypyrrole nanospheres were synthesized in the presence of HCl. The conductivity of these polypyrrole nanospheres is comparable to that of polypyrrole nanofibers reported elsewhere.[54] Note that the polymerization yield is only 2.7 wt % when polypyrrole was synthesized without an initiator, but increased to 42.6 wt % when 10 mol % initiator was added into the reaction. In addition, the polymerization yield was not affected by the choice of acid.

**Formation Mechanism of Polypyrrole Nanospheres.** Clearly, 2,4-diaminodiphenylamine plays a critical role in the formation of water-dispersible polypyrrole nano-

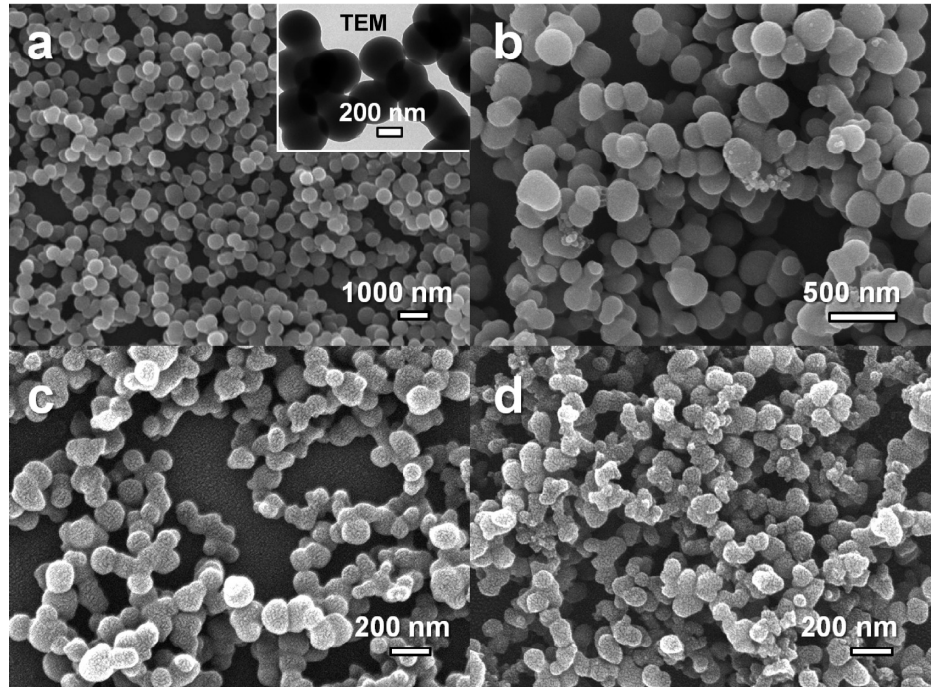


**Figure 5. SEM images of polypyrrole nanospheres synthesized with the following acids: (a) CSA, (b) $HClO_4$, (c) $HNO_3$, and (d) HCl using 10 mol % 2,4-diaminodiphenylamine initiator.**

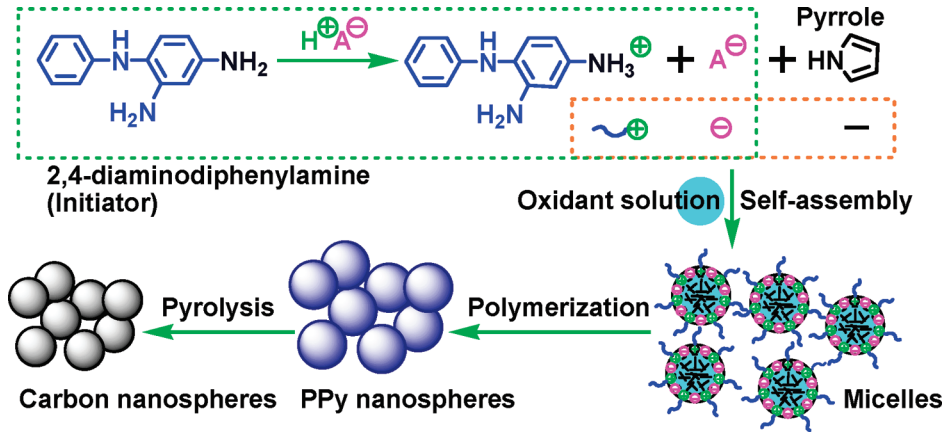


**Figure 6. Formation mechanism proposed for polypyrrole (PPy) and carbon nanospheres.**

spheres, and we believe it serves two functions. First, 2,4-diaminodiphenylamine has a much lower oxidation potential than pyrrole and thus it accelerates homogeneous nucleation of the polymerization reaction leading to polypyrrole chains. Perhaps even more importantly, 2,4-diaminodiphenylamine has two free amino groups, as illustrated in Figure 6, which can readily extract hydrogen ions from the added doping acid to form ammonium cations. This in turn makes the other side of the molecule, the diphenylamine, become hydrophobic with respect to the ammonium cations formed on the initiator. The hydrophilic ammonium cations and anions from the acid can then combine and self-assemble into nanomicelles stabilized by diphenylamine groups. That is to say, the initiator molecules act as a stabilizer for the as-formed nanomicelles. These nanomicelles likely act as templates to encapsulate pyrrole and oxidant leading to the formation of nanospheres during polymerization. When smaller size acids are employed, smaller diameter micelles are obtained leading to smaller sized polypyrrole nanospheres.

This proposed mechanism can be tested on a solution consisting of the initiator, acid, and methanol using dynamic light scattering (DLS). First, sonication was used in an attempt to dissolve 22.5 mg of the initiator in 15 mL of 1.0 M HCl, $HNO_3$, $HClO_4$, or CSA. The solutions exhibited soaplike bubbles when shaken. A 15 mL portion of methanol was then added to make sure all the initiators completely dissolved. This avoids errors caused by insoluble initiators when measured by DLS and decreases the size of the bubbles, which leads to micelles. As the size of the acid decreases, the average diameter of the micelles decreases from 872, to 729, to 525, and to 460 nm (Figure 7). Note that the diameter of the micelles are bigger than the corresponding polypyrrole nanosphere products, likely due to the pyrrole and oxidant incompletely filling the micelles during the encapsulation due to fluid dynamics. After polymerization, the materials consisting of monomer and oxidant will contract thus explaining why the diameter of the polymer nanospheres are smaller than that of the micelles. The DLS results thus provide strong support for the proposed nanosphere formation mechanism. Additionally, the acids used act as dopants. The smaller the size of the acid used, the tighter and smaller the diameters of the polypyrrole nanospheres produced. Different acids also change the solubility of the initiator and pyrrole oligomers, which also affect the diameters of the polypyrrole nanospheres. This confirms that the diameter of the micelles can be tuned by the choice of acid.

**Growth of Highly Conducting Carbon Nanospheres.** A high yield of carbon nanospheres can be directly produced by carbonization of the polypyrrole nanosphere precursors through pyrolysis. For example, when the polypyrrole nanospheres synthesized with HCl were pyrolyzed at 1100 °C for one hour, 50% of the polymeric nanospheres were converted into carbon-based materials, while the rest burned off as $CO_2$ and $H_2O$ along with HCl, $H_2$, $NH_3$, and $NO_2$. Powder XRD patterns indicate that the as-formed nanospheres are, in fact, partially crystalline carbon. The as-carbonized products show one sharp diffraction peak centered at $2\theta = 23.5°$ corresponding to the (002) reflection in turbostratic graphite (Figure 8). In addition, two new weak diffraction peaks centered at $2\theta = 43.5°$ and 79.5° emerge that can be assigned to the (101) and (110) Bragg reflections in graphite.[55−57] By comparing the powder XRD intensity of the (002) and (101) reflections of different carbon nanospheres, it appears that the smaller the size of the original polymer nanospheres, the higher the degree of carbonization. The increased peak intensity can be attributed to wider and thicker graphitic layers. The powder XRD patterns imply that the polypyrrole precursors have been converted into carbonaceous materials by pyrolysis. FT-IR spectra confirm that carbon-based materials have been, in fact, created since most of the characteristic peaks of the polymeric precursor disappear after carbonization (Figure S2).

Figure 9 panels a,b show SEM images of the carbon nanospheres formed at 800 °C from polypyrrole nano-

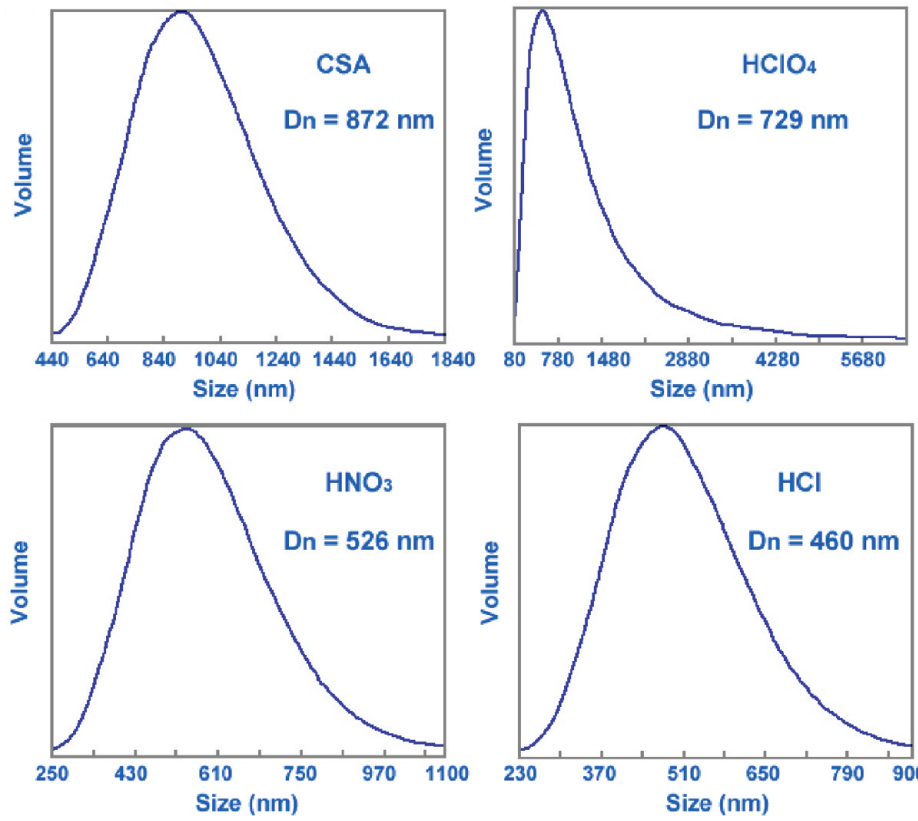


**Figure 7. Dynamic light scattering (DLS) spectra of the initiator-based micelles made from different sized acids.**

spheres synthesized in the presence of camphorsulfonic acid (CSA). Note that the nanospheres survive a direct heat treatment even up at 1100 °C (Figure 9c). When compared to the polymeric precursors, both SEM and TEM images show that the carbon nanospheres exhibit a similar morphology to that of the original polypyrrole nanospheres; except that the diameters have decreased by 20−30 nm due to dehydrogenation and aromatization shrinking the precursors. Apparently, the diameter, size distribution, and morphology of the carbon nanospheres are controlled by choosing different polypyrrole nanosphere precursors. For example, polypyrrole nanospheres synthesized using HCl and $HNO_3$ lead to polydispersed carbon nanospheres with small sizes of 50−80 and 90−100 nm (Figures 9c,d), respectively. However, polypyrrole nanospheres synthesized with camphorsulfonic acid (CSA) produce larger size (ca. 220 nm) but more well-defined carbon nanospheres, with a monodispersity as high as 95%, as determined by randomly examining 100 nanospheres. Interestingly, the as-formed carbon nanospheres, as well as the original polymer nanospheres, show excellent dispersibility in various polar solvents including ethanol, water, and toluene. The dispersibility of the carbon nanospheres at a low concentration (0.5 wt %) in ethanol was confirmed by both of SEM and TEM (Figure 9b), which demonstrate separate individual nanospheres of uniform size.

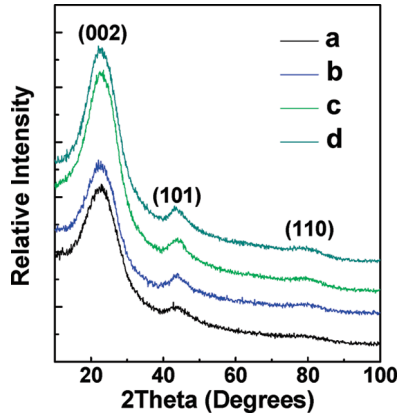


**Figure 8. XRD patterns of carbon nanospheres produced at 1100 °C from polypyrrole precursors synthesized with the following acids: (a) CSA, (b) $HClO_4$, (c) $HNO_3$, and (d) HCl.**

The reason that these nanostructures survive such a high temperature may be related to the chemical structure of polypyrrole. In the polymerization of pyrrole, there are α−α and α−β couplings of monomers which lead to linear and cross-linked polypyrrole, respectively.[58,59] When oxidants with higher oxidation potentials such as ferric chloride ($FeCl_3$), or ammonium peroxydisulfate (APS) are used, cross-linked polypyrrole consisting of rings of both pentagons and hexagons tend to form. We believe that these cross-linked structures are the principal reason that the sphere-like nanostructures survive the high temperature annealing. This also explains why polyaniline nanofibers synthe-

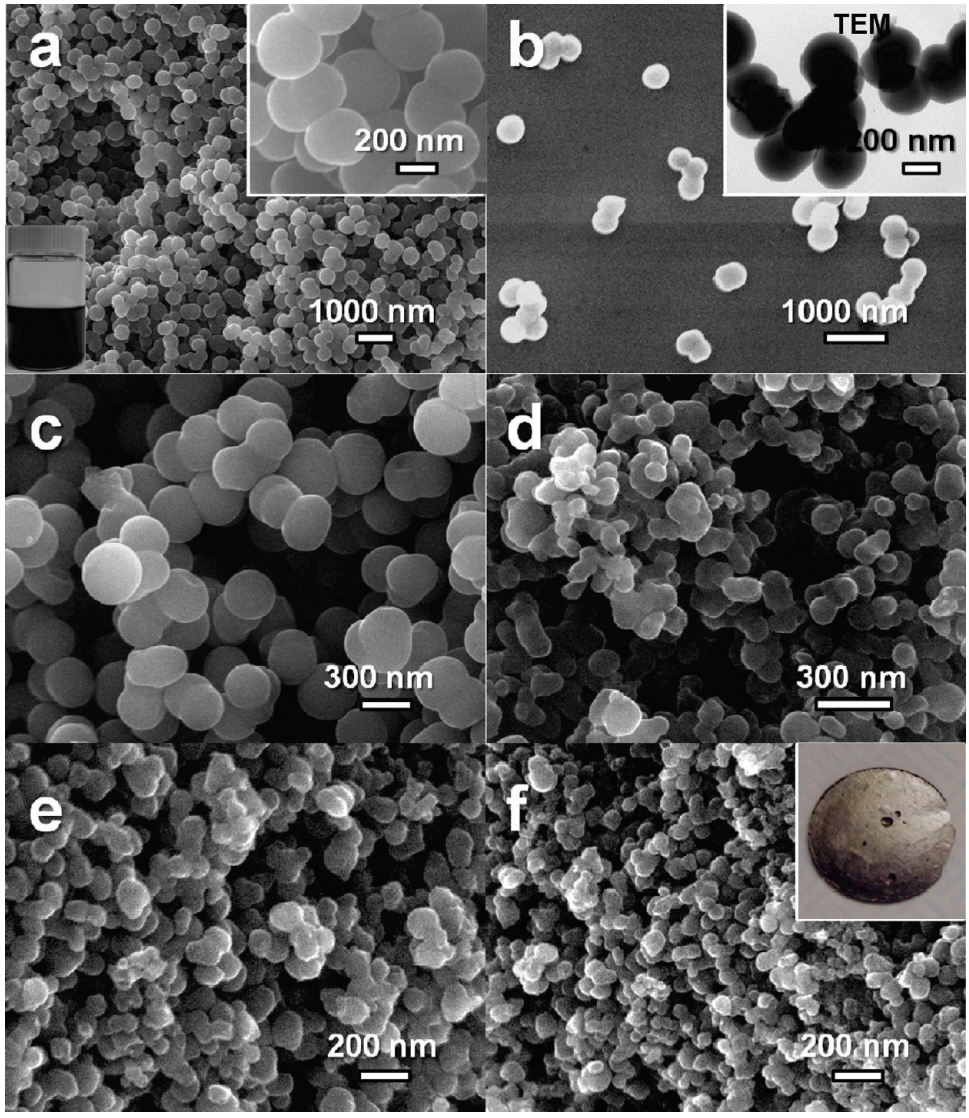


**Figure 9. SEM and TEM images of carbon nanospheres formed from polypyrrole nanospheres synthesized with the following acids: (a−c) CSA, (d) $HClO_4$, (e) $HNO_3$, and (f) HCl; the carbonization temperature for panels a and b was 800 °C and for panel c was 1100 °C. The insets show (a) a typical carbon nanosphere dispersion in ethanol (left bottom corner) and (f) a metal-like carbon nanosphere disk.**

sized from initiator polymerization,[48,60] due to their linear structures, could not survive high temperature (800 °C) carbonization (Supporting Information, Figure S3).

The as-formed carbon nanospheres created from the polypyrrole pyrolysis have very low electrical resistances. For example, when polypyrrole nanospheres synthesized with camphorsulfonic acid (CSA) were carbonized at 800 °C for half an hour, the sheet resistance of the as-formed carbon nanospheres was only 27 Ω/□, which is ~$10^3$ times lower than that of the corresponding polymer nanospheres. When the polymers were carbonized at a higher temperature (1100 °C) for a longer time (1 h), the sheet resistance of all the carbon nanospheres in pellet form was below 3 Ω/□. In particular, when polypyrrole nanospheres synthesized with HCl as the precursor were annealed at 1100 °C for 1 h, the sheet resistance of the as-formed carbon nanospheres was too low to measure using a two-point probe technique. The conductivity of this carbon material in the form of a metal-like disk is as high as 1180 S/cm as determined by a four-point probe technique, which is comparable to that of some metallic conductors such as mercury (conductivity = 1050 S/cm) and lead (conductivity = 1080 S/cm).[61] The conductivity of the carbon nanospheres is likely associated with the substitution of nitrogen atoms into the carbon structures. According to earlier work, when polypyrrole is carbonized above 900 °C, the nitrogen atoms are converted into two different types: pyridine-type nitrogen atoms (denoted $N_1$) and quarternary amine-type nitrogen atoms (denoted $N_2$), which according to X-ray photoelectron spectroscopy exist at the edge of graphene sheets (397.8 eV) and incorporate into the graphene sheets (400.7 eV), respectively.[62] These two types of nitrogen

atoms have also been reported for carbon nitrides and nitrogen enriched carbons.[63,64] Both experiments and theoretical calculations indicate that the electrical conduction in carbon materials can be enhanced by nitrogen atoms due to the introduction of donor states near the Fermi level.[65] The resistance of nitrogen atoms incorporated into a carbon lattice depends on the concentration of the nitrogen atoms as well as the $N_1/N_2$ ratio. In our case, elemental analysis indicates that the composition of the highly conducting carbon nanospheres is as follows: C (83.1 wt %), N (3.1 wt %), and H (1.7 wt %). This low concentration of substituted nitrogen atoms likely causes little distortion to the graphitic structure.[66] However, the doping effect of nitrogen atoms results in forming a new carbon-based material with the composition $CH_{0.24}N_{0.03}$. We believe that the nitrogen atoms play a critical role for markedly increasing the conductivity. The nitrogen atoms that remain in the carbon-based product may also help explain why the carbon nanospheres can be readily redispersed in water or ethanol since a charge stabilized colloid will result.

## CONCLUSIONS

Water-dispersible polypyrrole nanospheres have been successfully synthesized by simple chemical oxidative polymerization of pyrrole in the presence of 2,4-diaminodiphenylamine as an initiator. The morphology and size of the as-synthesized polypyrrole nanospheres are tunable by varying the initiator concentration, the oxidant used, and the acid employed. The initiator accelerates the rate of the polymerization reaction and forms nanomicelles which serve as templates leading to the formation of smooth and well-defined polypyrrole nanospheres. These nanospheres can be pyrolyzed at 1100 °C to form nitrogen-doped carbon nanospheres. The nanospheres are highly conducting with conductivity values up to 1180 S/cm. This simple and rapid synthesis provides a new route to produce water-dispersible conducting polymers and nitrogen-doped carbon nanospheres. We believe that the as-obtained conducting polymers and carbon nanospheres could find use in applications such as sensors, capacitors, and battery electrodes.

## EXPERIMENTAL SECTION

**Synthesis of Water-Dispersible Conducting Polymers Nanospheres.** In a typical synthesis of polypyrrole nanospheres, 25.0 mg of pyrrole and 7.5 mg of 2,4-diaminodiphenylamine (10 mol % relative to pyrrole) as an initiator were dissolved in methanol, while an oxidant such as $FeCl_3$ was dissolved in 1.0 mol/L HCl. The two solutions were cooled to 0 °C and rapidly mixed. The reaction was vigorously shaken for ~10 s and then left undisturbed overnight. The as-synthesized products were purified by centrifugation at a speed of 4500 rpm/min using DI water/methanol (90/10) at 15 °C until the top liquid became colorless. To monitor the polymerization of pyrrole, open-circuit potentials (OCP) of the reaction solutions were measured as a function of time on a single-component two-electrode cell: Pt|reaction solution‖reference electrode.[47,48] If not specifically mentioned, all experiments were performed using $FeCl_3$ as the oxidant and 10 mol % of 2,4-diaminodiphenylamine relative to pyrrole as an initiator.

**Growth of Carbon Nanospheres.** To produce carbon nanospheres, purified polypyrrole nanospheres in powder form were pyrolyzed in a furnace at a set temperature (*i.e.*, 800 or 1100 °C) at a ramp rate of 3 °C/min under an argon atmosphere. After carbonization at a set temperature, the furnace was cooled to room temperature at a rate of 3 °C/min.

**Characterization.** The chemical structure/composition of the purified polypyrrole and its carbon nanospheres were characterized by elemental analysis (EA) (performed by Columbia Analytical Services, Inc.). UV−vis absorption spectra were recorded on an HP 8453 spectrometer using samples prepared as dispersions in methanol. Solid state FT-IR samples were prepared as pellets by mixing with KBr, and the spectra were taken with a JASCO FT/IR-420 spectrometer. X-ray diffraction (XRD) patterns were scanned on a Philips X'pert Pro powder diffractometer by using copper-monochromatized CuKα radiation ($\lambda = 1.54178$ Å). The particle size distributions of the micelles formed by the initiator and acid, as well as polypyrrole methanol dispersions, were determined by a Coulter Beckman N4 Plus dynamic light scattering (DLS) analyzer. The electrophoretic mobility and zeta potential of polypyrrole particles were carried out at pH ~4.5 using a Brookhaven Instruments Corp. ZetaPALS. The morphologies of the polypyrrole and the as-formed carbon were imaged using a JEOL JSM-6700 field emission scanning electron microscope (SEM) and a PHILIPS CM120 transmission electron microscope (TEM).

**Electrical Measurements.** The resistances ($R_{sq}$) in ohms/square (Ω/□) of the polymer and carbon powder pellets were measured using a two-point probe set-up by painting two silver lines of the same length and sequence distance onto the surface; the relative error for these measurements is 10%. The resistivity of the carbon nanospheres prepared at 1100 °C for 1 h from polypyrrole synthesized using hydrochloric acid (HCl) as the dopant was measured by a four-point probe technique because its resistivity was too low to measure using the two-point probe.

*Acknowledgment.* The authors thank V. Strong for help with TEM, J. Wright for assistance with conductivity measurements, and T. Farrell for helpful discussions. Financial support from Abraxis Bioscience (RBK), the China Scholarship Council No. 2008626064 (Y.Z.L.), and National Natural Science Foundation of China (50773053) are gratefully acknowledged.

*Supporting Information Available:* UV-vis spectra of methanol dispersions; FT-IR analysis of carbon-based materials; polyaniline nanofiber control experiments. This material is available free of charge *via* the Internet at http://pubs.acs.org.

## REFERENCES AND NOTES

1. MacDiarmid, A. G. Synthetic Metals: A Novel Role for Organic Polymers (Nobel Lecture). *Curr. Appl. Phys.* **2001**, *1*, 269–279.
2. Janata, J.; Josowicz, M. Conducting Polymers in Electronic Chemical Sensors. *Nat. Mater.* **2003**, *2*, 19–24.
3. *Handbook of Conducting Polymers*; Skotheim, T. A., Reynolds, J. R., Eds.; CRC Press, Taylor & Francis Group: Boca Raton, FL, 2007.
4. Kudoh, Y. Properties of Polypyrrole Prepared by Chemical Polymerization Using Aqueous Solution Containing $Fe_2(SO_4)_3$ and Anionic Surfactant. *Synth. Met.* **1996**, *79*, 17–22.
5. Gilmore, K. J.; Kita, M.; Han, Y.; Gelmi, A.; Higgins, M. J.; Moulton, S. E.; Clark, G. M.; Kapsa, R.; Wallace, G. G. Skeletal Muscle Cell Proliferation and Differentiation on

Polypyrrole Substrates Doped with Extracellular Matrix Components. *Biomaterials* **2009**, *30*, 5292–5304.
6. Ramanaviciene, A.; Kausaite, A.; Tautkus, S.; Ramanavicius, A. Biocompatibility of Polypyrrole Particles: An *in-Vivo* Study in Mice. *J. Pharm. Pharmacol.* **2007**, *59*, 311–315.
7. Guimard, N. K.; Gomez, N.; Schmidt, C. E. Conducting Polymers in Biomedical Engineering. *Prog. Polym. Sci.* **2007**, *32*, 876–921.
8. Shi, W.; Liang, P.; Ge, D.; Wang, J.; Zhang, Q. Q. Starch-Assisted Synthesis of Polypyrrole Nanowires by a Simple Electrochemical Approach. *Chem. Commun.* **2007**, *23*, 2414–2416.
9. Jang, J.; Oh, J. H. A Facile Synthesis of Polypyrrole Nanotubes Using a Template-Mediated Vapor Deposition Polymerization and the Conversion to Carbon Nanotubes. *Chem. Commun.* **2004**, *7*, 882–883.
10. Cheng, D. M.; Xia, H. B.; Chan, H. S. O. Facile Fabrication of AgCl@Polypyrrole−Chitosan Core−Shell Nanoparticles and Polymeric Hollow Nanospheres. *Langmuir* **2004**, *20*, 9909–9912.
11. Zhang, X. Y.; Manohar, S. K. Narrow Pore-Diameter Polypyrrole Nanotubes. *J. Am. Chem. Soc.* **2005**, *127*, 14156–14157.
12. Mazur, M. Preparation of Surface-Supported Polypyrrole Capsules Using a Solidified Droplets Template Approach. *J. Phys. Chem. B* **2009**, *113*, 728–733.
13. Zhang, X. Y.; Manohar, S. K. Bulk Synthesis of Polypyrrole Nanofibers by a Seeding Approach. *J. Am. Chem. Soc.* **2004**, *126*, 12714–12715.
14. Yang, Y. S.; Liu, J.; Wan, M. X. Self-Assembled Conducting Polypyrrole Micro/Nanotubes. *Nanotechnology* **2002**, *13*, 771–773.
15. Huang, K.; Wan, M. X.; Long, Y. Z.; Chen, Z. J.; Wei, Y. Multi-functional Polypyrrole Nanofibers *via* a Functional Dopant-Introduced Process. *Synth. Met.* **2005**, *155*, 495–500.
16. Jang, J.; Oh, J. H.; Stucky, G. D. Fabrication of Ultrafine Conducting Polymer and Graphite Nanoparticles. *Angew Chem. Int. Ed.* **2002**, *41*, 4016–4019.
17. Zhang, X. T.; Zhang, J.; Liu, Z. F.; Robinson, C. Inorganic/Organic Mesostructure Directed Synthesis of Wire/Ribbon-like Polypyrrole Nanostructures. *Chem. Commun.* **2004**, *16*, 1852–1853.
18. Xu, P.; Han, X. J.; Zhang, B.; Mack, N. H.; Jeon, S.-H.; Wang, H.-L. Synthesis and Characterization of Nanostructured Polypyrroles: Morphology-Dependent Electrochemical Responses and Chemical Deposition of Au Nanoparticles. *Polymer* **2009**, *50*, 2624–2629.
19. Jang, J.; Yoon, H. Formation Mechanism of Conducting Polypyrrole Nanotubes in Reverse Micelle Systems. *Langmuir* **2005**, *21*, 11484–11489.
20. Jang, J.; Yoon, H. Facile Fabrication of Polypyrrole Nanotubes Using Reverse Microemulsion Polymerization. *Chem. Commun.* **2003**, *6*, 720–721.
21. Berdichevsky, Y.; Lo, Y. H. Polypyrrole Nanowire Actuators. *Adv. Mater.* **2006**, *18*, 122–125.
22. Antony, M. J.; Jayakannan, M. Amphiphilic Azobenzenesulfonic Acid Anionic Surfactant for Water-Soluble, Ordered, and Luminescent Polypyrrole Nanospheres. *J. Phys. Chem. B* **2007**, *111*, 12772–12780.
23. Kim, S. W.; Cho, H. G.; Park, C. R. Fabrication of Unagglomerated Polypyrrole Nanospheres with Controlled Sizes from a Surfactant-Free Emulsion System. *Langmuir* **2009**, *25*, 9030–9036.
24. Men'shikova, A. Y.; Shabsel's, B. M.; Evseeva, T. G. Synthesis of Polypyrrole Nanoparticles by Dispersion Polymerization. *Russ. J. Appl. Chem.* **2003**, *76*, 822–826.
25. Bocharova, V.; Kiriy, A.; Vinzelberg, H.; Mönch, I.; Stamm, M. Polypyrrole Nanowires Grown from Single Adsorbed Polyelectrolyte Molecules. *Angew. Chem., Int. Ed.* **2005**, *44*, 6391–6394.
26. Acik, M.; Baristiran, C.; Sonmez, G. Highly Surfaced Polypyrrole Nano-networks and Nano-fibers. *J. Mater. Sci.* **2006**, *41*, 4678–4683.
27. Dallas, P.; Niarchos, D.; Vrbanic, D.; Boukos, N.; Pejovnik, S.; Trapalis, C.; Petridis, D. Interfacial Polymerization of Pyrrole and *in Situ* Synthesis of Polypyrrole/Silver Nanocomposites. *Polymer* **2007**, *48*, 2007–2013.
28. Li, M.; Wei, Z. X.; Jiang, L. Polypyrrole Nanofiber Arrays Synthesized by a Biphasic Electrochemical Strategy. *J. Mater. Chem.* **2008**, *18*, 2276–2280.
29. Kroto, H. W.; Heath, J. R.; O'Brien, S. C.; Curl, R. F.; Smalley, R. E. $C_{60}$—Buckminsterfullerene. *Nature* **1985**, *318*, 162–163.
30. Iijima, S. Helical Microtubules of Graphitic Carbon. *Nature* **1991**, *354*, 56–58.
31. Hughes, T. V.; Chambers, C. R. Manufacture of Carbon Filaments. U.S. Patent 485, 615, 1892.
32. Krishnan, A.; Dujardin, E.; Treacy, M. M. J.; Hugdahl, J.; Lynum, S.; Ebbesen, T. W. Graphitic Cones and the Nucleation of Curved Carbon Surfaces. *Nature* **1997**, *388*, 451–454.
33. Sobkowicz, M. J.; Dorgan, J. R.; Gneshin, K. W.; Herring, A. M.; McKinnon, J. T. Renewable Cellulose Derived Carbon Nanospheres as Nucleating Agents for Polylactide and Polypropylene. *J. Polym. Environ.* **2008**, *16*, 131–140.
34. Jin, Y. Z.; Kim, Y. J.; Gao, C.; Zhu, Y. Q.; Huczko, A.; Endo, M.; Kroto, H. W. High Temperature Annealing Effects on Carbon Spheres and their Applications as Anode Materials in Li-Ion Secondary Battery. *Carbon* **2006**, *44*, 724–729.
35. Lee, K. T.; Lytle, J. C.; Ergang, N. S.; Oh, S. M.; Stein, A. Synthesis and Rate Performance of Monolithic Macroporous Carbon Electrodes for Lithium-Ion Secondary Batteries. *Adv. Funct. Mater.* **2005**, *15*, 547–556.
36. Lou, X. W.; Li, C. M.; Archer, L. A. Designed Synthesis of Coaxial $SnO_2$@Carbon Hollow Nanospheres for Highly Reversible Lithium Storage. *Adv. Mater.* **2009**, *21*, 2536–2539.
37. Wu, C. Z.; Zhu, X.; Ye, L. L.; Ouyang, C. Z.; Hu, S. Q.; Lei, L. Y.; Xie, Y. Necklace-like Hollow Carbon Nanospheres from the Pentagon-Including Reactants: Synthesis and Electrochemical Properties. *Inorg. Chem.* **2006**, *45*, 8543–8550.
38. Yan, A.; Lau, B. W.; Wessman, B. S.; Kulatos, I.; Yang, N. Y. C.; Kane, A. B.; Hurt, R. H. Biocompatible, Hydrophilic, Supramolecular Carbon Nanoparticles for Cell Delivery. *Adv. Mater.* **2006**, *18*, 2373–2378.
39. Oha, W. K.; Yoona, H.; Jang, J. Size Control of Magnetic Carbon Nanoparticles for Drug Delivery. *Biomaterials* **2010**, *31*, 1342–1348.
40. Ng, Y. H.; Ikeda, S.; Harada, T.; Higashida, S.; Sakata, T.; Mori, H.; Matsumura, M. Fabrication of Hollow Carbon Nanospheres Encapsulating Platinum Nanoparticles Using a Photocatalytic Reaction. *Adv. Mater.* **2007**, *19*, 597–601.
41. Miao, J. Y.; Hwang, D. W.; Narasimhulu, K. V.; Lin, L. P.; Chen, Y. T.; Lin, S. H.; Hwang, L. P. Synthesis and Properties of Carbon Nanospheres Grown by CVD Using Kaolin Supported Transition Metal Catalysts. *Carbon* **2004**, *42*, 813–822.
42. Calderón-Moreno, J. M.; Labarta, A.; Batlle, X.; Pradell, T.; Crespo, D.; Binh, V. T. Magnetic Properties of Dense Carbon Nanospheres Prepared by Chemical Vapor Deposition. *Chem. Phys. Lett.* **2007**, *447*, 295–299.
43. McKinnon, J. T.; Herring, A. M.; McCloskey, B. D. Laser Pyrolysis Method for Producing Carbon Nano-spheres. U.S. Patent 7,601,321 B2, 2009.
44. Bystrzejewski, M.; Lange, H.; Huczko, A.; Baranowski, P.; Hübers, H.-W.; Gemming, T.; Pichler, T.; Büchner, B.; Rümmeli, M. H. One-Step Catalyst-Free Generation of Carbon Nanospheres *via* Laser-Induced Pyrolysis of Anthracene. *J. Solid State Chem.* **2008**, *181*, 2796–2803.
45. Qiao, W. M.; Song, Y.; Lim, S. Y.; Hong, S. H.; Yoon, S. H.; Mochida, I.; Imaoka, T. Carbon Nanospheres Produced in an Arc-Discharge Process. *Carbon* **2006**, *44*, 187–190.
46. Xia, Y. D.; Yang, Z. X.; Mokaya, R. Mesostructured Hollow Spheres of Graphitic N-Doped Carbon Nanocast from Spherical Mesoporous Silica. *J. Phys. Chem. B* **2004**, *108*, 19293–19298.

47. Tran, H. D.; Shin, K.; Hong, W. G.; D'Arcy, J. M.; Kojima, R. W.; Weiller, B. H.; Kaner, R. B. A Template-free Route to Polypyrrole Nanofibers. *Macromol. Rapid Commun.* **2007**, *28*, 2289–2293.
48. Tran, H. D.; Wang, Y.; D'Arcy, J. M.; Kaner, R. B. Toward an Understanding of the Formation of Conducting Polymer Nanofibers. *ACS Nano* **2008**, *2*, 1841–1848.
49. Zhang, W. X.; Wen, X. G.; Yang, S. H. Synthesis and Characterization of Uniform Arrays of Copper Sulfide Nanorods Coated with Nanolayers of Polypyrrole. *Langmuir* **2003**, *19*, 4420–4426.
50. Li, X. G.; Wei, F.; Huang, M. R.; Xie, Y. B. Facile Synthesis and Intrinsic Conductivity of Novel Pyrrole Copolymer Nanoparticles with Inherent Self-Stability. *J. Phys. Chem. B* **2007**, *111*, 5829–5836.
51. Zhang, X.; Zhang, J.; Song, W.; Liu, Z. Controllable Synthesis of Conducting Polypyrrole Nanostructures. *J. Phys. Chem. B* **2006**, *110*, 1158–1165.
52. *Ionic Hydration in Chemistry and Biophysics*; Conway, B. E., Eds.; Elsevier Scientific Publishing Company: New York, 1981.
53. Lee, K.-H.; Park, B. J.; Song, D. H.; Chin, I.-J.; Choi, H. J. The Role of Acidic *m*-Cresol in Polyaniline Doped by Camphorsulfonic Acid. *Polymer* **2009**, *50*, 4372–4377.
54. Goela, S.; Mazumdara, N. A.; Gupta, A. Synthesis and Characterization of Polypyrrole Nanofibers with Different Dopants. *Polym. Adv. Tech.* **2009**, *21*, 205–210.
55. Xu, L. Q.; Zhang, W. Q.; Yang, Q.; Ding, Y. W.; Yu, W. C.; Qian, Y. T. A Novel Route to Hollow and Solid Carbon Spheres. *Carbon* **2005**, *43*, 1090–1092.
56. Li, Z. Q.; Lu, C. J.; Xia, Z. P.; Zhou, Y.; Luo, Z. X-ray Diffraction Patterns of Graphite and Turbostratic Carbon. *Carbon* **2007**, *45*, 1686–1695.
57. Jang, J.; Li, X. L.; Oh, J. H. Facile Fabrication of Polymer and Carbon Nanocapsules Using Polypyrrole Core/Shell Nanomaterials. *Chem. Commun.* **2004**, *7*, 794–795.
58. Kim, S. W.; Park, C. R. Catalyst-free and Template-free Preparation of Semi-cylindrical Carbon Nanoribbons. *Carbon* **2009**, *47*, 2391–2395.
59. *Conjugated Polymers and Related Materials*; Salaneck, W. R., Lundström, I., Rånby, B., Eds.; Oxford University Press: London, 1993.
60. Li, W. G.; Wang, H.-L. Oligomer-Assisted Synthesis of Chiral Polyaniline Nanofibers. *J. Am. Chem. Soc.* **2004**, *126*, 2278–2279.
61. Ricou, R.; Vives, C. Local Velocity and Mass Transfer Measurements in Molten Metals Using an Incorporated Magnet Probe. *Int. J. Heat Mass Transfer* **1982**, *25*, 1579–1588.
62. Wang, Y.; Su, F. B.; Wood, C. D.; Lee, J. Y.; Zhao, X. S. Preparation and Characterization of Carbon Nanospheres as Anode Materials in Lithium-Ion Secondary Batteries. *Ind. Eng. Chem. Res.* **2008**, *47*, 2294–2300.
63. Derradji, N. E.; Mahdjoubi, M. L.; Belkhir, H.; Mumumbila, N.; Angleraud, B.; Tessier, P. Y. Nitrogen Effect on the Electrical Properties of $CN_x$ Thin Films Deposited by Reactive Magnetron Sputtering. *Thin Solid Films* **2005**, *482*, 258–263.
64. Hou, P. X.; Orikasa, H.; Yamazaki, T.; Matsuaka, K.; Tomita, A.; Setoyama, N.; Fukushima, Y.; Kyotani, T. Synthesis of Nitrogen-Containing Microporous Carbon with a Highly Ordered Structure and Effect of Nitrogen Doping on $H_2O$ Adsorption. *Chem. Mater.* **2005**, *17*, 5187–5193.
65. Lee, S. U.; Belosludov, R. V.; Mizuseki, H.; Kawazoe, Y. Designing Nanogadgetry for Nanoelectronic Devices with Nitrogen-Doped Capped Carbon nanotubes. *Small* **2009**, *5*, 1769–1775.
66. Cruz-Silva, E.; Lopez-Urias, F.; Munoz-Sandoval, E.; Sumpter, B. G.; Terrones, H.; Charlier, J. C.; Meunier, V.; Terrones, M. Electronic Transport and Mechanical Properties of Phosphorus- and Phosphorus-Nitrogen-Doped Carbon Nanotubes. *ACS Nano* **2009**, *3*, 1913–1921.